ACS Macro Letters

Letter

pubs.acs.org/macroletters

Omniphobic Slippery Coatings Based on Lubricant-Infused Porous Polyelectrolyte Multilayers

Xiayun Huang,[†] James D. Chrisman,[†] and Nicole S. Zacharia*[,†,‡]

[†]Department of Mechanical Engineering and [‡]Department of Materials Science and Engineering, Texas A&M University, College Station, Texas 77843, United States

Supporting Information

ABSTRACT: Omniphobic and slippery coatings from lubricant-infused, textured surfaces have recently been shown to have superior properties including low contact angle hysteresis and low sliding angles. Here, we present an omniphobic slippery surface prepared by infusing a fluorinated lubricant into a porous polyelectrolyte multilayer. These surfaces repel water and decane with sliding angles as low as 3°. One advantage of polyelectrolyte multilayers is the ease with which they can coat nonplanar surfaces, demonstrated here.

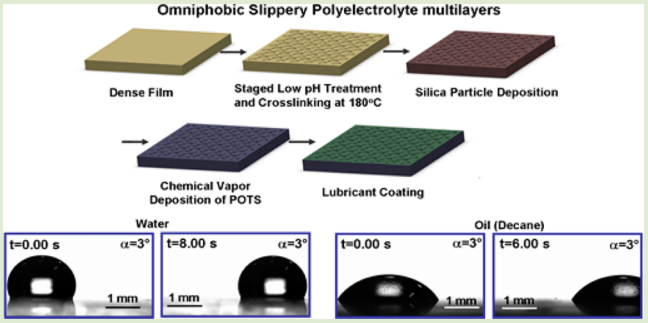

Omniphobic and nonfouling coatings have many different potential uses, ranging as widely as energy savings from suppression of frost formation or improved aerodynamics to increased product lifetimes by the resistance of biofouling or staining.[1−6] While the lotus leaf structure (a rough surface with a combination of micro- and nanoscaled features) has been the inspiration for many superhydrophobic coatings, these surfaces have some limitations due to the fact that they rely on trapped air pockets.[7] Because of this reliance on air pockets it has been found that humidity, temperature, and pressure can all damage these lotus leaf structures.[7−10] Also, they are not necessarily able to repel low surface energy liquids.[8] More recently, a class of lubricant-infused surfaces based on the structure of the pitcher plant has been shown to have superior properties for repelling all types of liquids.[1−6,11,12] These surfaces have been named slippery liquid infused porous surfaces (or SLIPS), and their properties include very low sliding angles and low contact angle hysteresis.[1] Simply put, the requirements for making a SLIPS are to start with a textured surface that will wick the lubricant into it and that will preferentially wet the lubricant compared to the liquids to be repelled, and the liquids to be repelled should be immiscible with the lubricant.[1]

We present here a new approach to the fabrication of these omniphobic slippery surfaces by the use of polyelectrolyte multilayers (PEMs) assembled by the layer-by-layer (LbL) technique. LbL is a sequential assembly technique that directs the complexation of oppositely charged polyelectrolytes onto a surface.[13] The method has a strong track record of being a robust and versatile platform for fabrication of films with a wide range of functionality,[14] including superhydrophobic[15] and olephobic surfaces.[16] For other SLIPS or lubricant-infused polymer surfaces, the textured surfaces are defined by lithographic means,[1,9] deposited electrochemically which requires a conductive substrate,[6] or require an adhesion layer.[2,11] Many commercially available textured substrates cannot be applied to curved surfaces. Polyelectrolyte multilayers provide advantages in these respects; they take advantage of a bottom-up assembly process, and the charge groups of the polymer chains (especially for amine-containing polymers) act as their own adhesion layer.

In this work, water-soluble weak polyelectrolytes, branched poly(ethylene imine) (BPEI) and poly(acrylic acid) (PAA), were used as the basis for the polyelectrolyte multilayer structure. These weak polyelectrolytes have a variable charge density based on changes in protonation that accompany variations in the pH of the surrounding environment. Exposing these films to changes in pH after assembly can create the formation of pores,[17] and the resultant porous structure is dependent on both the pH the films are exposed to after assembly as well as the initial assembly pH. Honeycomb-like microporous structures can be achieved through staged acid treatment. A semifluorinated silane treatment creates superhydrophobicity from an otherwise hydrophilic polyelectrolyte multilayer. Infusing the surface with lubricant gives a perfect film with omniphobic slippery properties allowing the drops to exist in a Cassie state. These surfaces repel water and decane with sliding angles as low as 3° and with contact angle hysteresis lower than 2°. An advantage of using a polyelectrolyte multilayer is the ease with which they can coat curved surfaces and those with more complex geometries without the need for additional adhesion layers.

We have previously found that multilayers assembled from branched poly(ethyleneimine) (BPEI) and poly(acrylic acid)

Received: July 24, 2013
Accepted: August 28, 2013
Published: September 4, 2013

(PAA) with the BPEI assembly solution at pH 9.5 and the PAA assembly solution at pH 4.5 formed porous structures with pore size ranging from very large to submicrometer.[18] Postassembly acid treatment in this case creates pores much smaller than postbase treatment.[18] Recently, we have studied the possible pore sizes and window of pH stability and how they are influenced by both the pH value of postassembly treatment solution and the pH values of the assembly solutions.

BPEI has a branched structure containing primary, secondary, and tertiary amine groups in a ratio of 25%, 50%, and 25%, respectively.[19] The pK_a values for the different amine groups are 4.5 for primary, 6.7 for secondary, and 11.6 for tertiary amine groups.[20] Moreover, highly branched structures mean denser coils as compared to linear polymers. The pK_a of PAA is roughly 5.5−6.5.[21] At a pH value of 4.5, PAA is only partially charged, but there is still sufficient charge to form polyelectrolyte multilayers. $(BPEI/PAA)_{30}$ films (assembly pH 9.5, 7.5, and 6.5 for BPEI and assembly pH 4.5 for PAA) as assembled here are all over 2.5 um, shown in Figure S1 (Supporting Information).

When immersed into post-treatment solutions of varying pH values for 1 h, porous features are seen for both the acid and base ranges due to the change of solubility and rearrangement of the charged polymer chains and the release of some polyelectrolyte chains from the film.[17,22,23] Under exposure to solutions with pH intermediate to the values of the original assembly solutions, the film is stable, showing a smooth surface and retaining nearly 100% of the original film thickness. Figure 1 shows that the stable range for $BPEI_{9.5}/PAA_{4.5}$ films is from pH 4 to pH 9, which is similar to the pH values of the assembly solutions (pH 9.5 for BPEI and pH 4.5 for PAA). A noticeable decrease in the pH stability window to pH 5−pH 6 is seen when the assembly pH of BPEI is decreased from 9.5 to 6.5. This kind of film with a narrow stability window can be

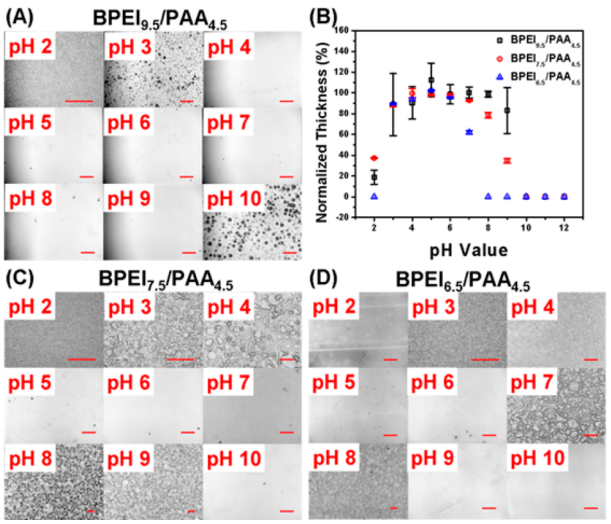

Figure 1. pH window over which a BPEI/PAA film is stable when immersed in solutions of varying pH. Optical micrographs of porous structures of $(BPEI/PAA)_{30}$ film after postassembly treatment in different pH solutions for 1 h. Assembly pH of PAA was kept as 4.5, while that of BPEI was 9.5, 7.5, or 6.5 as shown in (A), (C), and (D). (B) Normalized film thicknesses of dried $(BPEI/PAA)_{30}$ film with different assembly pH immersed in varying pH solutions for 1 h. The window of stability is always in between the assembly pH of BPEI and PAA and becomes narrow when the BPEI assembly pH is decreased to 6.5. The scale bar for all the micrographs is 200 μm.

decomposed much more easily and quickly compared to those films with a broad stability window. An important distinction is that the film itself is decomposing, not the polymer chains within the film. When the pH of BPEI is as high as 9.5, the charge density of the polymer is relatively low (Figure S2, Supporting Information), and the polymer chains become more coiled. The resultant multilayer structure contains less PAA, and those PAA chains have a higher charge density as compared to solution (Figure S3, Supporting Information). Such a film deposits in thick layers due to the BPEI conformation, and the multilayer has many loops and unbound functional groups (Figure S1, Supporting Information).[21] A higher BPEI charge density (low assembly pH), however, results in a more extended conformation and thinner layers. Postassembly treatments will change the polyelectrolyte charge densities within the films, causing morphological rearrangements. We hypothesize that when BPEI is deposited in a more extended conformation (higher charge density) the resultant film is more readily dissolved with changes in the external environment due to lower levels of diffusion and entanglement between the film components.

The different assembly conditions combined with different postassembly processes are found to result in different types of porous structures. In this work, we focus on the microscale and submicrometer-sized pores created by postassembly acid treatment, giving us the optimal microstructure for our application. Optical micrographs from Figure 1 show the range of structures possible. BPEI/PAA films with assembly pH value for BPEI of 6.5 result in the finest pore features. Here we have chosen $BPEI_{6.5}/PAA_{4.5}$ films as the optimal multilayer system to manipulate the pore size and features by staged acid treatment.

Rubner et al.[15,24] have studied microporous formation and report that PAH/PAA films can be induced to form pores on the order of 10 μm with honeycomb-like structures and submicrometer pores on the surface by using an appropriate combination of postacid treatments, a process we call staged acid treatment. $BPEI_{6.5}/PAA_{4.5}$ films behave similarly and can form both micrometer and submicrometer pore sizes with staged acid treatment of pH 2.7 and pH 2.3. Figure 2 shows the SEM images of a porous $BPEI_{6.5}/PAA_{4.5}$ film throughout the staged acid treatment. The first solution at pH 2.7 forms pores about 10 μm in size. These honeycomb-like structures can be formed at short immersion times, such as 10 min. This is much faster than PAH/PAA films, which require a few hours to achieve honeycomb-like porous structures.[24] The pores become deeper when the pH 2.7 solution treatment time is increased to 30 min. Further treatment with a more acidic solution of pH 2.3 bites into the submicrometer pores at the boundaries of the honeycomb-like structures created with the pH 2.7 treatment. By increasing the exposure time in the pH 2.3 solution, the honeycomb-like structures will eventually be destroyed (Figure 2, pH 2.7/10 min−pH 2.3/30 min; pH 2.7/30 min−pH 2.3/20 min), and in some cases when exposure in the lower pH solution is sufficiently long the structure is restored to a smooth surface (Figure 2, pH 2.7/30 min−pH 2.3/30 min).

Here, we have chosen staged acid treatment conditions (pH 2.7 for 30 min and pH 2.3 for 10 min) for polyelectrolyte SLIPS fabrication. The porous $BPEI_{6.5}/PAA_{4.5}$ film based on these staged acid etching conditions gives both the microscaled and submicrometer porous features, which we have found to be the optimal structure for the purpose of a slippery and omniphobic surface, as shown in Figure 3(A). The porous film

dx.doi.org/10.1021/mz400387w | ACS Macro Lett. 2013, 2, 826−829

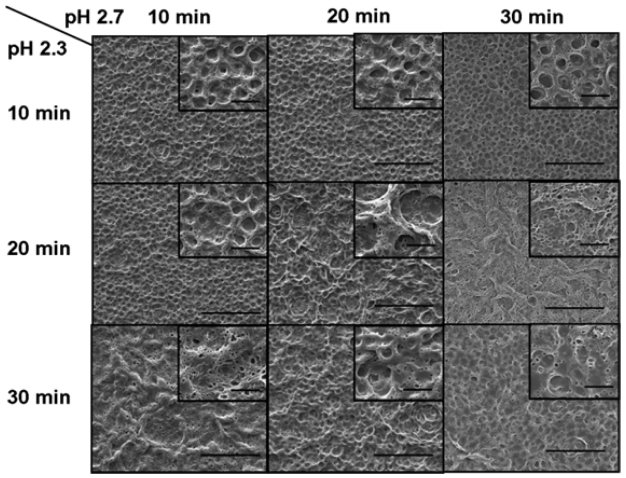

Figure 2. SEM images of porous structures of $(BPEI_{6.5}/PAA_{4.5})_{30}$ films that evolve through staged acid treatment. The insets in each image are high magnification SEM images of the porous structures. The scale bars for the low magnification and high magnification images are 100 and 20 μm, respectively. The corresponding size and distribution of both the large microscaled pores and the smaller nanoscaled pores are shown in Table S1 (Supporting Information).

was thermally cross-linked at 180 °C for 2 h to fix the porous structures for the further dipping and reaction procedures.[15,24] Nanoscale roughness was introduced through a further three bilayers dip coating of BPEI and silica nanoparticles (a mixture of 20 and 4 nm particle dispersion).[25] Porous structures with micro- and nanoscale roughness features are achieved by this step. Although there are reports that nanoscaled roughness as opposed to a hierarchically structured material is adequate to create a SLIPS surface,[2] we have found that the hierarchical surface optimizes our coating's properties. This may be due to the increased surface area for deposition of the nanoparticles that is made available by using a porous polyelectrolyte multilayer instead of a flat one. The rough film surface is then made to be superhydrophobic through a chemical vapor deposition (CVD) of POTS at 120 °C for 3 h.[25] The reaction was performed in a closed-capped weighing bottle as shown in Figure 3(B), and POTS reacted with hydroxyl groups from the silica nanoparticles to form a hydrophobic molecularly thin layer. The CVD step transforms the hydrophilic porous film to a superhydrophobic one with a water contact angle of 157.8°, illustrated in Figure 3(C). This film is further coated with a low surface energy lubricant by spin-coating that actually reduces the water contact angle (118.9°) but gives the porous film an excellent liquid repellency to both water and oil. Figure 3(D) shows the advancing and receding angles of both water and decane droplets when the droplet is sliding at a 3° tilting angle. The SLIPS film repels both the polar (water) and nonpolar liquids (decane). They start sliding at a very low tilting angle (~3°) and move off the screen which is 5 mm in width within a few seconds as shown in Figure 3(E). This process can be seen in the movies in the Supporting Information (mz400387w_si_002.mpg and mz400387w_si_003.mpg). The contact angle hysteresis for both polar and nonpolar liquids is very low (<2°) for drop volume as small as 5 μL.

The robustness of the films regarding temperature was also investigated. Similar to the lotus leaf, the porous polyelectrolyte multilayer system used here is hydrophilic itself, but the addition of a thin hydrophobic layer can be used to obtain superhydrophobicity. It has been reported[26] that 55 °C hot water can wash off the hierarchical roughness and wax surface layer (with its melting point around 40−50 °C) of the lotus leaf and ruin its hydrophobicity. Most artificial lotus leaf structures with either hydrophilic or hydrophobic bulk properties exhibit worse performance regarding water contact angle at water temperatures over 55 °C, as the surface tension of water is reduced at higher temperature.[26] SLIPS systems retain their high water contact angle and slippery properties when touched with high-temperature water.[15] Although the polyelectrolyte multilayer system chosen here has hydrophilic properties before our processing,[27] it can repel water and oil after having been

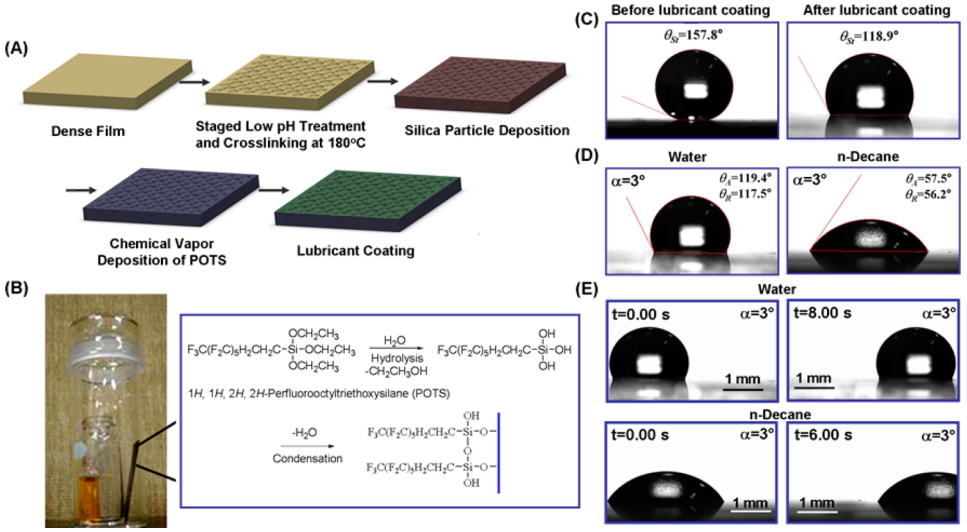

Figure 3. Design and omniphobicity of SLIPS from polyelectrolyte multilayers. (A) Schematics of the procedure for fabricating SLIPS from $(BPEI_{6.5}/PAA_{4.5})_{30}$ film. (B) The setup used for chemical vapor deposition (CVD) of POTS (the liquid in the vial has been colored to orange for ease of visualization) with a proposed reaction of POTS. (C) Static contact angles of a 5 μL water drop on the film surface before and after lubricant coating. (D) Optical micrograph of the advancing and receding angle of water and decane (5 μL), which are captured at the droplets slide on the polyelectrolyte SLIPS with a tilting angle of 3.0°, showing a contact angle hysteresis lower than 2°. (E) Optical micrographs demonstrating the mobility of water and decane droplets (5 μL) sliding on a SLIPS at a low titling angle (α = 3.0°).

dx.doi.org/10.1021/mz400387w | ACS Macro Lett. 2013, 2, 826−829

coated with a thin layer of a low surface energy lubricant, and slippery properties can be maintained for both water and oil from 25 to 95 °C (shown in Figure S5(A), Supporting Information). The sliding properties remain similar when the multilayer is chilled to −10 °C, shown in the Supporting Information (mz400387w_si_006.mpg).

Another advantage of working with polyelectrolyte multilayers is the ease with which they can coat curved surfaces with molecular level adhesion (no other type of adhesion layer required). The curved surface chosen here, a glass tube as shown in Figure S5(B and C) (Supporting Information), can be coated with the same procedures described above. Figure S5(B) shows water dyed with methylene blue (the lower phase) and a mixture of decane with silicone oil (the oil added for color) as the upper phase in the beaker. Figure S5(C) has oil and water phases inverted, and the heavy oil phase used is chloroform. The polyelectrolyte SLIPS on the glass tube can repel water, decane, and chloroform without any droplets adhering to the tube's surface, while the bare glass tube itself will become coated with an adhesion layer, especially the blue dyed water. This can be better visualized by watching the movies in the Supporting Information (mz400387w_si_004.mpg and mz400387w_si_005.mpg). Furthermore, with its low sliding angles, our film is truly a self-cleaning surface. A supplemental movie (Supporting Information, mz400387w_si_007.mpg) shows silica powder being sprinkled on both our polyelectrolyte SLIPS and a superhydrophobic polyelectrolyte film (our same film without the lubricant) and then water droplets being used to roll the dust off of the film. It is clear that the low sliding angle helps in this process enormously.

We have demonstrated a new method for fabrication of slippery, omniphobic coatings based on a textured polyelectrolyte multilayer. Our materials are repellant to both oil and water with sliding angles of 3° and extremely low contact angle hysteresis of 2°. These films work over a range of temperatures and are still slippery in an environment where water has condensed on the film. The low sliding angles make these surfaces truly self-cleaning. Polyelectrolyte multilayers are inherently simple to coat on curved surfaces regardless of radius of curvature, and the polyelectrolyte SLIPS coating is demonstrated on a glass tube.

■ ASSOCIATED CONTENT

Supporting Information

Materials and methods, Figures S1−S5, Table S1, and movies. This material is available free of charge via the Internet at http://pubs.acs.org.

■ AUTHOR INFORMATION

Corresponding Author

*E-mail: nzacharia@tamu.edu.

Notes

The authors declare no competing financial interest.

■ ACKNOWLEDGMENTS

The authors thank the Texas A&M University and the Texas A&M Engineering Experiment Station for start-up funds as well as partial support from NSF CAREER DMR-1255612. The authors acknowledge the Microscopy and Imaging Center (MIC) at Texas A&M University for access to the FE-SEM. The FE-SEM instrument was supported by the National Science Foundation under Grant DBI-0116835. The authors also thank Dr Karen L. Wooley for use of her FTIR instrument.

■ REFERENCES

(1) Wong, T. S.; Kang, S. H.; Tang, S. K. Y.; Smythe, E. J.; Hatton, B. D.; Grinthal, A.; Aizenberg, J. *Nature* **2011**, *477*, 443.
(2) Kim, P.; Kreder, M. J.; Alvarenga, J.; Aizenberg, J. *Nano Lett.* **2013**, *13*, 1793.
(3) Howard, A. S. *ACS Nano* **2012**, *6*, 6536.
(4) Nishimoto, S.; Bhushan, B. *RSC Adv.* **2013**, *3*, 671.
(5) Epstein, A. K.; Wong, T. S.; Belisle, R. A.; Boggs, E. M.; Aizenberg, J. *Proc. Natl. Acad. Sci. U.S.A.* **2012**, *109*, 13182.
(6) Kim, P.; Wong, T. S.; Alvarenga, J.; Kreder, M. J.; Adorno-Martinez, W. E.; Aizenberg, J. *ACS Nano* **2012**, *6*, 6569.
(7) Quéré, D. *Annu. Rev. Mater. Res.* **2008**, *38*, 71.
(8) Bocquet, L.; Lauga, E. *Nat. Mater.* **2011**, *10*, 334.
(9) Smith, J. D.; Dhiman, R.; Anand, S.; Reza-Garduno, E.; Cohen, R. E.; McKinley, G. H.; Varanasi, K. K. *Soft Matter* **2013**, *9*, 1772.
(10) Daniel, D.; Mankin, M. N.; Belisle, R. A.; Wong, T. S.; Aizenberg, J. *Appl. Phys. Lett.* **2013**, *102*, 231603−1.
(11) Yao, X.; Hu, Y.; Grinthal, A.; Wong, T. S.; Mahadevan, L.; Aizenberg, J. *Nat. Mater.* **2013**, *12*, 529.
(12) Wilson, P. W.; Lu, W.; Xu, H.; Kim, P.; Kreder, M. J.; Alvarenga, J.; Aizenberg, J. *Phys. Chem. Chem. Phys.* **2013**, *15*, 581.
(13) Decher, G.; Schlenoff, J. B. *Multilayer Thin Film*; Wiley-VCH: Weinheim, Germany, 2003.
(14) Hammond, P. T. *Adv. Mater.* **2004**, *16*, 1271.
(15) Zhai, L.; Berg, M. C.; Cebeci, F. C.; Kim, Y.; Milwid, J. M.; Rubner, M. F.; Cohen, R. E. *Nano Lett.* **2006**, *6*, 1213.
(16) Aulin, C.; Yun, S. H.; Wagberg, L.; Lindstrom, T. *ACS Appl. Mater. Interfaces* **2009**, *1*, 2443.
(17) Mendelsohn, J. D.; Barrett, C. J.; Chan, V. V.; Pal, A. J.; Mayes, A. M.; Rubner, M. F. *Langmuir* **2000**, *16*, 5017.
(18) Huang, X.; Schubert, A. B.; Christman, J. D.; Zacharia, N. S. *Langmuir* **2013**, submitted for publication.
(19) Shiro, K.; Kazuhisa, H.; Masazumi, T.; Takeo, S. *Macromolecules* **1987**, *20*, 1496.
(20) Willner, I.; Eichen, Y.; Frank, A. J.; Fox, M. A. *J. Phys. Chem.* **1993**, *97*, 7264.
(21) Choi, J.; Rubner, M. F. *Macromolecules* **2005**, *38*, 116.
(22) Wang, X.; Liu, F.; Zheng, X.; Sun. *Angew. Chem., Int. Ed.* **2011**, *50*, 11378.
(23) Hiller, J.; Mendelsohn, J. D.; Rubner, M. F. *Nat. Mater.* **2002**, *11*, 59.
(24) Zhai, L.; Cebeci, F. C.; Cohen, R. E.; Rubner, R. F. *Nano Lett.* **2004**, *4*, 1349.
(25) Li, Y.; Li, L.; Sun, J. *Angew. Chem., Int. Ed.* **2010**, *49*, 6129.
(26) Liu, Y.; Chen, X.; Xin, J. H. *J. Mater. Chem.* **2009**, *19*, 5602.
(27) Bravo, J.; Zhai, L.; Wu, Z.; Cohen, R. E.; Rubner, M. F. *Langmuir* **2007**, *23*, 7293.